

tmp title: MUSC source

Damien Pageot^{*†}, Donatienne Leparoux^{*}, Mathieu Le Feuvre^{*}, Olivier

Durand^{*} and Yann Capdeville[†]

^{*}*LUNAM-IFSTTAR*,

[†]*OSUNA*

^{*}*LPGN*,

(May 7, 2015)

GEO-Example

Running head: *Geophysics* example

ABSTRACT

INTRODUCTION

Since decades, geophysicists develop numerical imaging methods for seismic measurements to determine the structures and the physical properties of the Earth at several scales as subsurface (civil engineering), crustal, regional or global. These methods, like Full Waveform Inversion (FWI), are still in development and are mostly validated using synthetic data which are generally computed using the same wave propagation modeling engine used in the inverse problem process. In other terms, the synthetic data are computed with some assumptions (for example acoustic approximation or two-dimensional) which are the same in the inverse problem. Although, this *inverse crime* (Wirgin, 2004) is particularly useful to validate an algorithm in its early development stage, it does not allow to assess the efficiency of the method for real seismic data. Moreover, because no one known precisely the Earth interior, it is difficult to evaluate the capacity of a method to recover physical parameters and structures from real seismic data. Thus, it is necessary to add a step for which imaging methods will be tested for experimental seismic measurements obtained under controlled conditions.

The best way to satisfy this need is to use Small Scale Modeling Methods (SSMM). SSMM were used since several years to study the propagation of waves in various media with several stage of complexity, from acoustic wave propagation in homogeneous media to elastic wave propagation in three-dimensional heterogeneous media (Rieber, 1936; Howes et al., 1953; Hilterman, 1970; French, 1974; Bishop et al., 1985; Pratt, 1999), and allow to generate experimental seismic data under well-controlled conditions. Some methods exist to produce this kind of data for different purpose and the MUSC Laboratory (Bretaudeau et al., 2008, 2011, 2013), *Mesure Ultrasonore Sans Contact* in French, in one of them. MUSC is designed

to allow (1) wide-angle on-shore acquisitions modeling both body waves and surface waves, (2) automatic multisource-multireceiver measurements with a high-productivity, (3) high-precision source-receiver positioning and (4) high-precision recording of absolute surface displacement without coupling effects.

Our objective here is to increase the potential of the MUSC system as a reliable tool for generating experimental data which will be distributed in the scientific community. Thus we present two studies of experimental data in order to : 1) refine the comparison between numerical and experimental data by taking into account the 2D/3D effects through an alternative way and 2) identify the reproducibility of the source impact. These approaches complete the knowledge of the system and facilitate the achievement of massive multi-source and multi-receiver data simulating subsurface seismic experimental campaigns.

To achieve these objectives, we used a seismic wave modeling code based on the Spectral Element Method (Komatitsch et al., 1998; Komatitsch and Tromp, 1999; Komatitsch et al., 2005; Festa and Vilotte, 2005). This method has several advantages compared to finite differences and finite elements, such as: (1) a weak formulation which can naturally take into account the free surface, (2) an explicit scheme in time facilitating parallelization and reducing the computational cost, (3) a spatial discretization (mesh) convenient for the representation of complex environments and (4) high precision results and low numerical dispersion.

Describe the principal results of the investigation...

METHODS

Physical modeling: MUSC Bench

The MUSC bench (Bretaudeau et al., 2008, 2011, 2013) is built to experimentally reproduce field seismic data with a great accuracy on small scale model 1. The bench is composed of a honeycomb tab and two arms which control the source and the receiver position with a precision of $10\text{ }\mu\text{m}$.

The receiving system of MUSC Laboratory is composed of a laser interferometer. The principle of this laser is based on a phase shift of the reflected laser signal due to the wave propagation in the material. A real-time calibration value enables a continuous conversion to a nanometric displacement. The focal diameter of the laser on the model surface is about several micrometers and allows a detection limit of 2.5 nm in the frequency range from 30 kHz to 20 MHz.

The seismic source is simulated by a piezoelectric transducer that allows to modify the waveform as required, *i.e.*, Gauss source, Ricker source, etc. The source is generated by a waveform generator and is then amplified before transducing to the small-scale-model.

For the purpose of small scale modeling, the change of scale must keep the relationship between observables. For most of seismic imaging methods, the significant physical parameters are the compressional and shear waves velocities, V_P and V_S respectively, the density ρ and the quality factor Q . When scaling the model, many parameters can be modified: the distances, the time scale, the amplitudes of the signals, the visco-elastic properties, etc. Hence, the predominant factor is the wavelength $\lambda = V/f$, where V is the wave velocity and f the frequency. Thus, physical and mechanical parameters are modified to preserve the

ratio $\lambda_{real} = \xi \lambda_{scale}$ where ξ is the scale ratio. It is therefore necessary to act directly on the time-frequency scales. Assuming the materials used to build the small scale model have the same mechanical properties (V_P , V_S , ρ) than the natural media, it is straightforward to obtain the scale ratios for parameters involved in seismic experiment.

For near surface experiments, the scale ratio ξ is about 1000 which means that the central frequency f_0 of the source is few kHz (generally 100 kHz but can be more or less), distances are in mm (acquisition length around 50 mm typically) and time unit is ms .

Small-scale models are generally made of metal, thermoplastic or melted epoxy resin-based materials (Bretaudière et al., 2013, 2011, 2008). These materials allow to reproduce complex geometries and have a large panel of physical and mechanical properties. These materials have the advantages to have physical properties closed to natural soil materials. The models are generally oversized to easily separate reflected waves on boundaries from the rest of the signal.

Numerical modeling: Spectral Element Method

Various numerical methods exist to resolve the equation of motion in arbitrary elastic media. The most widely used is the Finite-Differences (FD) method (Virieux, 1986; Levander, 1988; Robertsson et al., 1994; Pratt, 1990; Stekl and Pratt, 1998; Saenger and Bohlen, 2004) which estimates each derivative on a regular cartesian grid using a Taylor development (Moczo et al., 2004) of order n . FD is simple to implement but quickly shows some limitations: the cartesian grid is defined by the minimum propagated wavelength (λ_{min}) in the full media and is unable to reproduce properly complex topography and interfaces. Moreover, Saenger et al. (2000) show that 60 points by wavelength (λ) are needed to modelise

Rayleigh wave in order $n = 2$ where only 15 points by λ are required for body waves which increases drastically the numerical cost in case of near-surface modeling experiment. The Finite-Elements Method (FEM) is another popular method used for wave propagation modeling. FEM is based on a variationnal formulation of the equation of motion and gives a continuous approximate solution in space using polynomial basis functions defined on each node of each cell of the mesh. The natural boundary conditions of FEM is the free surface and the triangular (in 2D) or tetraedric (in 3D) unstructured meshes are well adapted to complex media and topography. However, low polynomial basis are inadequate with fine spatial discretisation and the required discretisation to obtain precise and non-dispersive solution is numerically costly.

Recently, the Spectral Element Method (SEM), used in fluid dynamics, was adapted to seismic wave propagation. SEM proposes to resolve the partial derivative system of the local equation of motion using a variationnal formulation of the problem. FEM allows structured and unstructured meshes using quadrangular cells in 2D and hexaedral cells in 3D. Basically, SEM is a FEM developed on Legendre polynomial basis. The solution is constructed on Gauss-Lobatto-Legendre (gll) quadratic rules which allows a spectral convergence ratio with the increase of interpolation order. The spectral convergence ratio allows a weak numerical dispersion and the quadrangular (in 2D) and hexaedral (in 3D) meshes are well adapted to most configuration and topography.

As in FEM, all boundary of the domain are reflecting and the free surface is the natural condition. In order to simulate infinite or semi-infinite domain, SEM uses PML conditions (Bérenger, 1994; Festa and Vilotte, 2005).

RESULTS

From point-source to line-source acquisition

In the framework of wave propagation modeling and waveform inversion, most of available algorithms are limited to the two-dimensional approximation especially for computational cost causes. Thus, line-source seismograms are required as observed data to be compared to synthetic seismograms or for inversion processes.

However, MUSC is designed to produce three-dimensional experimental seismograms from a piezo-electric source selected to be as closed as possible to a point source. Generally, the correction of the geometrical spreading is done by convolving each trace by $\sqrt{t^{-1}}$, where t is the traveltime, with or without offset conditioning. The correct phase can then be obtained using a source wavelet estimation method (Bretaudeau et al., 2011).

Recently, Forbriger et al. (2014) and Schafer et al. (2014) have developed, and successfully applied to synthetic seismogram, an hybrid method to convert the three-dimensional geometrical spreading in two-dimensional spreading using both convolution tapering and offset dependent scaling of the waveform. However, these pre-processing methods are not perfect and can not be easily automated and the results are strongly conditioned by user's experience and attempts.

Here, we take advantage of the experimental framework to explore an alternative approach specific to MUSC. Contrary to field experiments, it is possible to generate a pseudo-line-source finely sampled by multiple point-sources, perpendicular to the acquisition line. The line-source, along the y-axis, is sampled by 481 point-sources spaced of 0.5 mm. Four source-receiver offsets are considered: 90, 95, 100 and 105 mm. Each receiver is perpendicular to

and centered on the line-source. For each receiver position, the complete signal is stacked along source position to obtain an equivalent two-dimensional line-source response.

Figures 3(a,b,c,d) show the comparison between experimental traces obtained using a point-source and a line-source for 90, 95, 100 and 105 mm offset respectively. Even if waveforms seem quite similar, amplitude differences and phase shifts between point-source and line-source responses may be critical in a two-dimensional FWI process as shown by Schafer et al. (2014).

Figures 3(e,f,g,h) show the comparison between experimental traces using a line-source and a point-source after geometrical spreading corrections.

These results show that the line-source emulation on the MUSC laboratory is efficient and can produce data suitable for imaging methods such as 2D FWI.

Experimental source reproducibility

To assess the ability of MUSC to provide reproducible data, *i.e.* to evaluate the reproducibility of the source impact, several physical modeling were performed on a homogeneous epoxy-resin block for which the seismic waves velocities and the intrinsic attenuation are known : $V_P = 2300 \text{ m.s}^{-1}$, $V_S = 1030 \text{ m.s}^{-1}$, $\rho = 1300 \text{ kg.m}^{-3}$ and $Q = 30$.

Six realizations have been acquired on this model with a similar geometry setup, *i.e.* 121 receivers positions with an increment equal to 1 mm and a minimum offset of 10 mm. The numerical wavelet sent to the piezzo-electric transducer source is a Ricker signal with a central frequency of 100 kHz. However, the source waveform is modified by the physical coupling effect of the transducer.

First, source wavelet were estimated for each experiment (Figure 4(a)). The effective sources show different oscillations after the main pulse, due to internal echoes in the transducer. These secondary oscillations have a very similar shape from an experiment to another, as well as the global signal shape even if some small differences of amplitudes appear for the main pulse. Figure 4(b,c,d,e,f,g) show numerically propagated signals after convolution with estimated source wavelets for the offset of 60 mm. The corrected numerical seismograms are in good agreement with the experimental seismograms. The value of the correlation coefficient (> 0.98 , also presented in the figure) confirms the great efficiency of the wavelet source assessment process.

In a second step, a unique source wavelet is estimated by taking into account the 6 experiments together (figure 5(a)). The resulting source parameters were applied to the synthetic signals (figure 5(b,c,d,e,f,g)) for the same receiver position as previously. As in the previous case, the corrected seismograms are in good agreement with the experimental seismograms (correlation coefficients > 0.96).

These last results, based on an average estimated source wavelet show that the effective impulse source emitted by the transducer in the MUSC measurement bench is stable enough to ensure a robust reproducibility of the source. Therefore, concerning the key issue of the source knowledge, experimental data acquired in the MUSC laboratory can be efficiently processed by imaging methods like Full Waveform Inversion (FWI) with only one estimation step for all the multi-source and multi-receivers data.

CONCLUSIONS

These two studies allow to refine the capacity of the physical modeling designed for seismic experiments simulation by 1) completing the validation of the measurement through comparison of numerical and experimental data generated by a realistic 2D source line and 2) assessing the reproductivity of the effective source emitted in a model. These improvements allow to provide and distribute experimental reduced scale data to the scientific community as benchmark datasets.

PLOTS

Equations

Figures

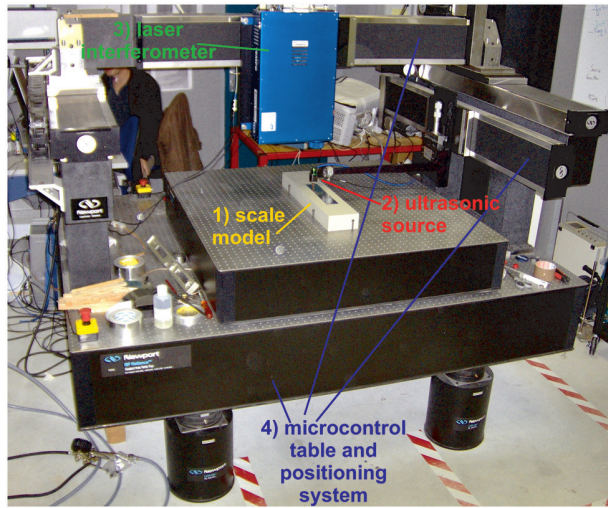


Figure 1: Photograph of the MUSC ultrasonic laboratory (from Bretaudeau et al. (2013)) with its four components: (1) a small-scale model of the underground, (2) an optical table with two automated arms moving above the model, (3) a laser interferometer recording ultrasonic wave propagation at the model surface, and (4) a piezoelectric ultrasonic source generating ultrasonic waves in the model.

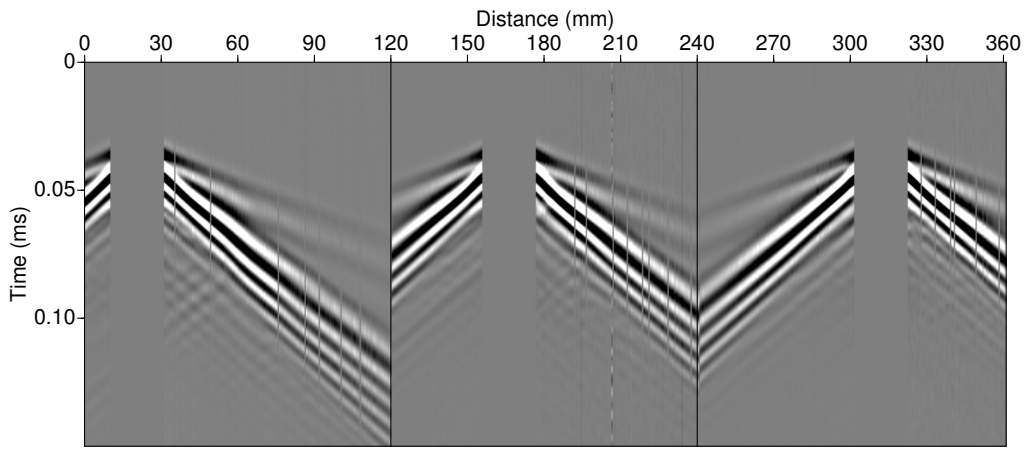


Figure 2: Example of multi-source multi-receiver record on the MUSC bench for a two-layer model (balt).

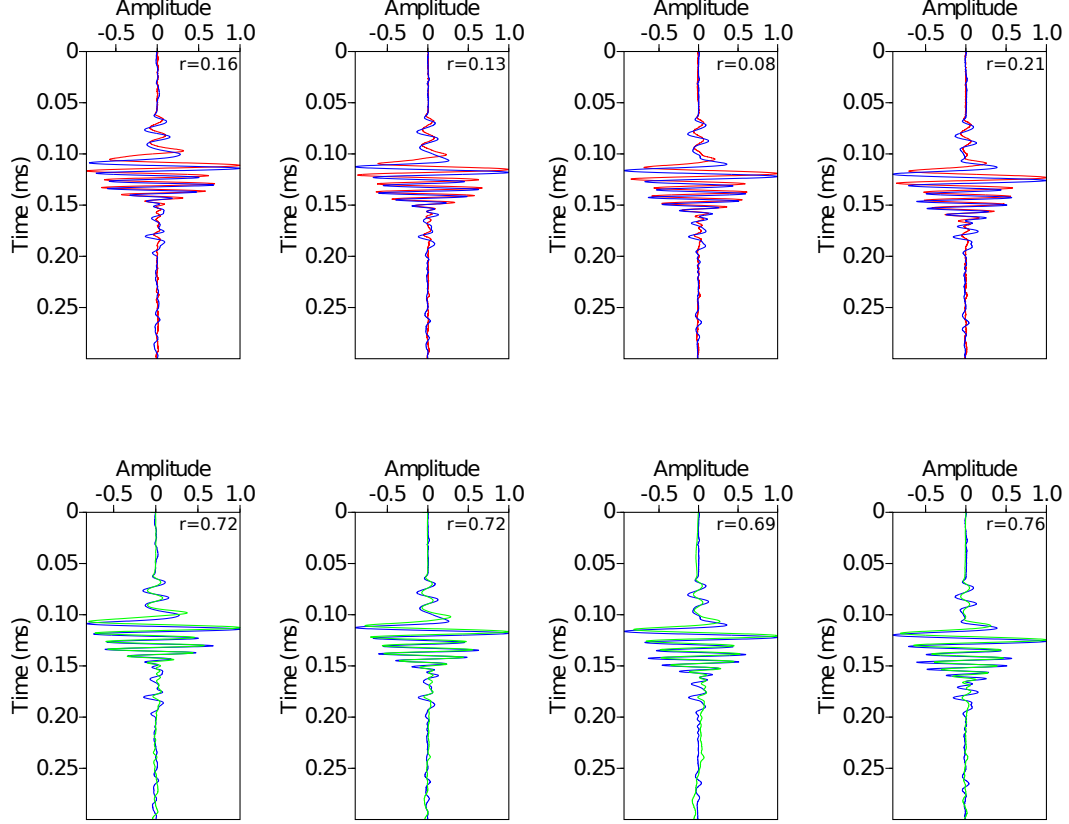


Figure 3: (a,b,c,d) Comparison between an experimental seismogram for a point-source (red), an experimental seismogram for a line-source (blue) for 90, 95, 100 and 105 mm offset respectively. (e,f,g,h) Comparison between an experimental seismogram for a line-source (blue), and for a point-source corrected from geometrical spreading (green) for 90, 95, 100 and 105 mm offset respectively r gives the correlation factor between numerical simulation from the estimated effective source and experimental traces.

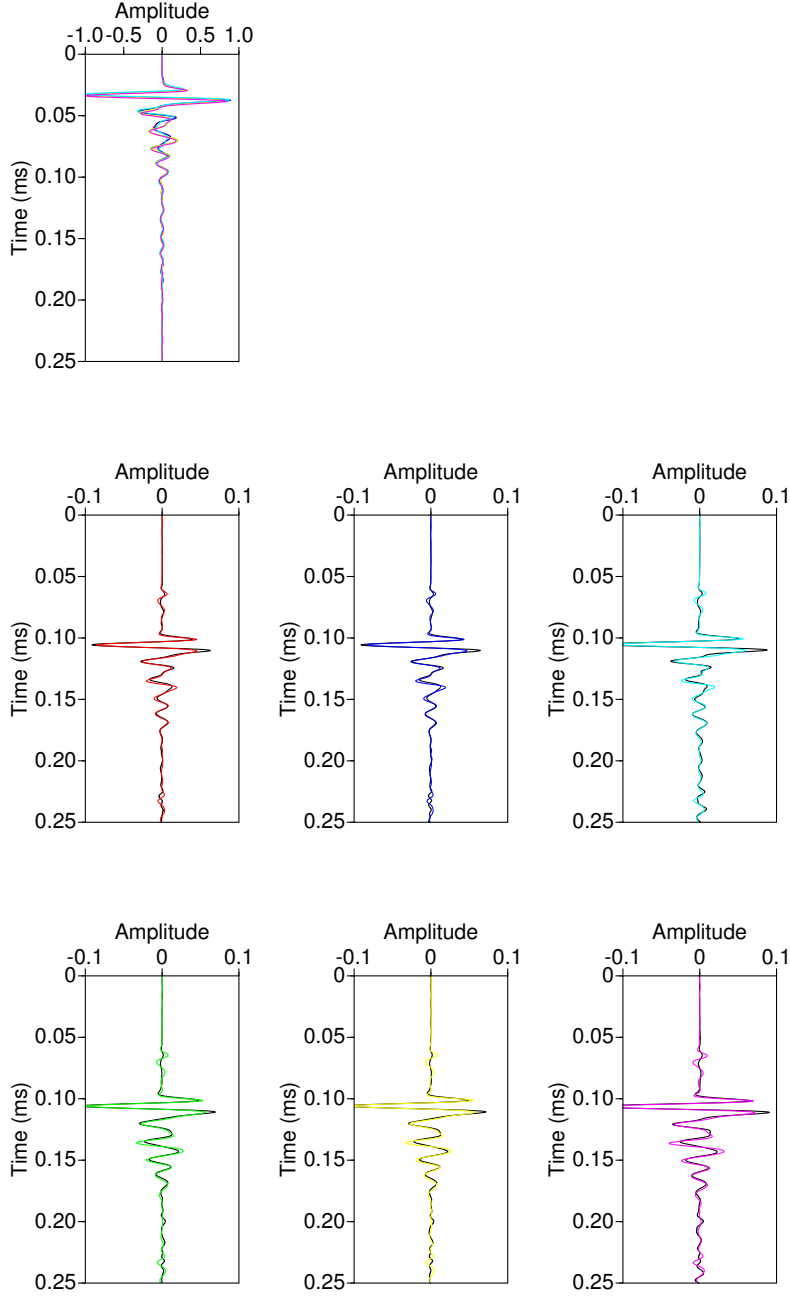


Figure 4: (a) Comparison between six estimated source wavelets (ESW) calculated for each experiment. (b,c,d,e,f,g) Comparison between experimental traces (black) and numerically simulated traces corrected with the corresponding estimated effective source (colored). \mathbf{r} gives the correlation factor between numerical simulation from the estimated effective source and experimental traces.

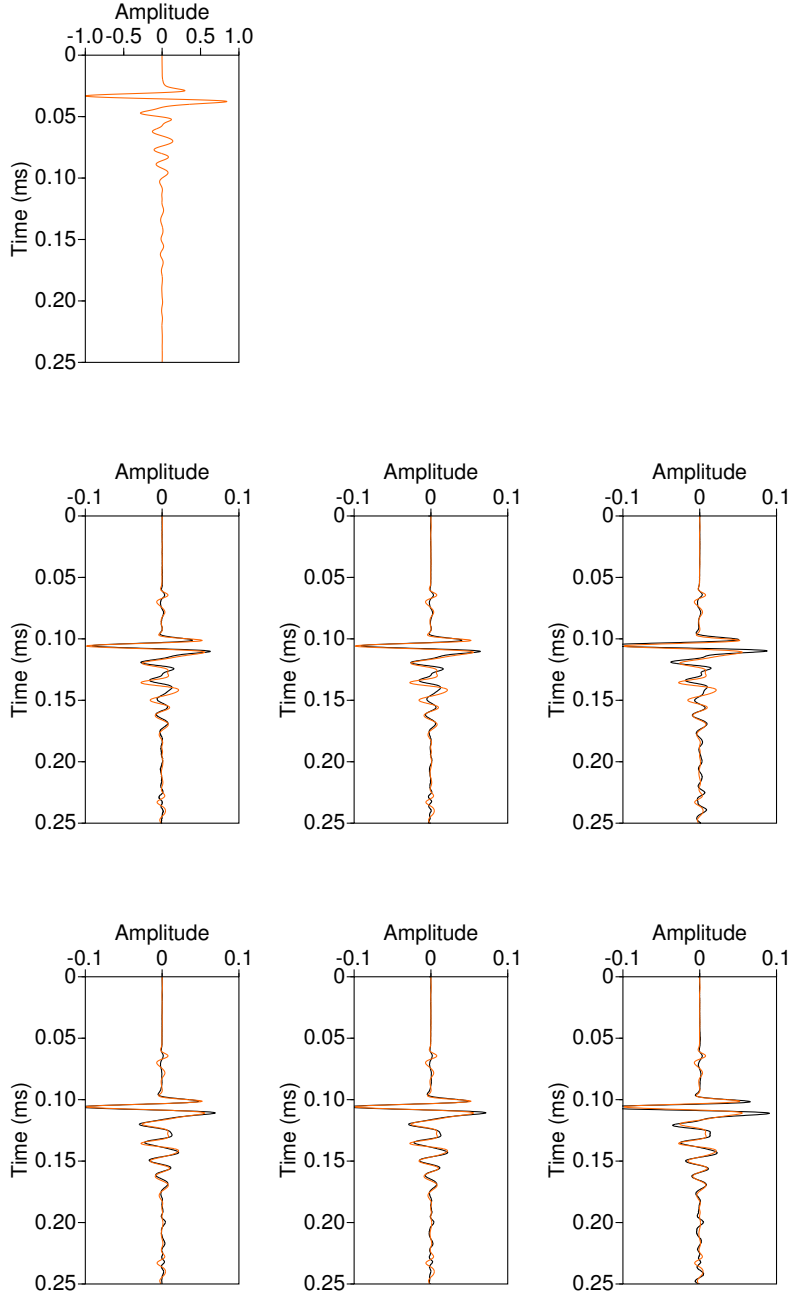


Figure 5: (a) Estimated source wavelet (*ESW*) calculated for all experiments. (b,c,d,e,f,g,h) Comparison between experimental traces (black) and numerically simulated traces corrected with the corresponding estimated effective source (colored). \mathbf{r} gives the correlation factor between numerical simulation from the estimated effective source and experimental traces.

Tables

ACKNOWLEDGMENTS

REFERENCES

- Bérenger, J. P., 1994, A perfectly matched layer for the absorption of electromagnetic waves: Journal of Computational Physics, **114**, 185–200.
- Bishop, T., K. Bube, R. Cutler, R. Langan, P. Love, J. Resnick, R. Shuey, and D. Spinder, 1985, Tomographic determination of velocity and depth in laterally varying media: Geophysics, **50**, 903–923.
- Bretaudeau, F., R. Brossier, D. Leparoux, O. Abraham, and J. Virieux, 2013, 2d elastic full-waveform imaging of the near-surface: application to synthetic and physical modelling data sets: Near Surface Geophysics.
- Bretaudeau, F., D. Leparoux, and O. Abraham, 2008, Small scale adaptation of the seismic full waveform inversion method - application to civil engineering applications.: The Journal of the Acoustical Society of America, **123**.
- Bretaudeau, F., D. Leparoux, O. Durand, and O. Abraham, 2011, Small-scale modeling of onshore seismic experiment: A tool to validate numerical modeling and seismic imaging methods: Geophysics, **76(5)**, T101–T112.
- Festa, G., and J. Vilotte, 2005, The Newmark as velocity-stress time-staggering: an efficient PML implementation for spectral element ssimulation of elastodynamics: Geophysical Journal International, **161**, 798–812.
- Forbriger, T., L. Gross, and M. Schafer, 2014, Line-source simulation for shallow-seismic data.part 1: Theoretical background: Geophysical Journal International.
- French, W., 1974, Two-dimensional and three-dimensional migration of model-experiment reflection profiles: Geophysics, **39**, 265–277.
- Hilterman, F., 1970, Three-dimensional seismic modeling: Geophysics, **35**, 1020–1037.
- Howes, E., L. Tejada-Flores, and L. Randolph, 1953, Seismic model study: Journal of the

- Acoustical Society of America, **25**, 915–921.
- Komatitsch, D., and J. Tromp, 1999, Introduction to the spectral-element method for three-dimensional seismic wave propagation: *Geophysical Journal International*, **139**, 806–822.
- Komatitsch, D., S. Tsuboi, and J. Tromp, 2005, The spectral-element method in seismology.
- Komatitsch, D., J. P. Vilotte, R. Vai, J. M. Castillo-Covarrubias, and F. J. Sánchez-Sesma, 1998, The Spectral Element Method for Elastic Wave Equation: Application to 2-D and 3-D Seismic Problems: *International Journal for Numerical Methods in Engineering*, **45**, 1139–1164.
- Levander, A., 1988, Fourth-order finite-difference p-sv seismograms: *Geophysics*, **53**, 1425–1436.
- Moczo, P., J. Kristek, and L. Halada, 2004, The finite-differences method for seismologists: An introduction: Comenius University, Bratislava.
- Pratt, R. G., 1990, Frequency domain elastic wave modeling by finite differences: A tool for cross-hole seismic imaging.: *Geophysics*, **55**, 626–632.
- , 1999, Seismic waveform inversion in the frequency domain, Part 1: Theory and verification in a physical scale model: *Geophysics*, **64**, 888–901.
- Rieber, F., 1936, Visual presentation of elastic wave patterns under various structural conditions: *Geophysics*, **1**, 196–218.
- Robertsson, J., J. Blanch, and W. Symes, 1994, Viscoelastic finite-difference modeling.: *Geophysics*, **59**, 1444–1456.
- Saenger, E. H., and T. Bohlen, 2004, Finite-difference modeling of viscoelastic and anisotropic wave propagation using the rotated staggered grid: *Geophysics*, **69**, 583–591.
- Saenger, E. H., N. Gold, and A. Shapiro, 2000, Modeling the propagation of elastic waves using a modified finite-difference grid: *Wave Motion*, **31**, 77–92.

- Schafer, M., L. Gross, T. Forbriger, and T. Bohlen, 2014, Line-source simulation for shallow-seismic data. part2: full-waveform inversion – a synthetic 2-d case study: *Geophysical Journal International*, **198**, 1405–1418.
- Stekl, I., and R. G. Pratt, 1998, Accurate visco-elastic modeling by frequency-domain finite differences, using rotated operators.: *Geophysics*, **63**, 1779–1794.
- Virieux, J., 1986, P-sv wave propagation in heterogeneous media: velocity-stress finite-difference method: *Geophysics*, **51**, 889–901.
- Wirgin, A., 2004, The inverse crime: *ArXiv Mathematical Physics e-prints*. (Provided by the SAO/NASA Astrophysics Data System).